TOXICOLOGICAL SCIENCES **117(1)**, 180–189 (2010)
doi:10.1093/toxsci/kfq176
Advance Access publication June 16, 2010

γ-Diketone Axonopathy: Analyses of Cytoskeletal Motors and Highways in CNS Myelinated Axons

Lihai Zhang,* Terrence Gavin,† Anthony P. DeCaprio,‡ and Richard M. LoPachin*,[1]

*Department of Anesthesiology, Albert Einstein College of Medicine, Montefiore Medical Center, Bronx, New York 10467-2490; †Department of Chemistry, Iona College, New Rochelle, New York 10804; and ‡Department of Chemistry and Biochemistry, Florida International University, Miami, Florida 33199

[1]To whom correspondence should be addressed at Montefiore Medical Center, Moses Research Tower-7, 111 East 2210th Street, Bronx, NY 10467-2490. Fax: (718) 515-4903. E-mail: lopachin@aecom.yu.edu.

Received April 23, 2010; accepted June 8, 2010

2,5-Hexanedione (HD) intoxication is associated with axon atrophy that might be responsible for the characteristic gait abnormalities, hindlimb skeletal muscle weakness and other neurological deficits that accompany neurotoxicity. Although previous mechanistic research focused on neurofilament triplet proteins (NFL, NFM, NFH), other cytoskeletal targets are possible. Therefore, to identify potential non-NF protein targets, we characterized the effects of HD on protein-protein interactions in cosedimentation assays using microtubules and NFs prepared from spinal cord of rats intoxicated at different daily dose rates (175 and 400 mg/kg/day). Results indicate that HD did not alter the presence of α- or β-tubulins in these preparations, nor were changes noted in the distribution of either anterograde (KIF1A, KIF3, KIF5) or retrograde (dynein) molecular motors. The cosedimentation of dynactin, a dynein-associated protein, also was not affected. Immunoblot analysis of microtubule-associated proteins (MAPs) in microtubule preparations revealed substantial reductions (45–80%) in MAP1A, MAP1B heavy chain, MAP2, and tau regardless of HD dose rate. MAP1B light chain content was not altered. Finally, HD intoxication did not influence native NF protein content in either preparation. As per previous research, microtubule and NF preparations were enriched in high–molecular weight NF species. However, these NF derivatives were common to both HD and control samples, suggesting a lack of pathognomonic relevance. These data indicate that, although motor proteins were not affected, HD selectively impaired MAP-microtubule binding, presumably through adduction of lysine residues that mediate such interactions. Given their critical role in cytoskeletal physiology, MAPs could represent a relevant target for the induction of γ-diketone axonopathy.

Key Words: **γ-diketone neuropathy; axonal cytoskeleton; neurofilament; microtubule-associated proteins; protein adduct; axon atrophy.**

Exposure of laboratory animals to 2,5-hexanedione (HD) or the parent hexacarbons, *n*-hexane, or methyl *n*-butyl ketone, produces axon atrophy in peripheral nervous system (PNS) and central nervous system (CNS) (Lehning *et al*., 1995, 2000; LoPachin *et al*., 1994, 2003; reviewed in LoPachin and Lehning, 1997 and LoPachin and DeCaprio, 2004). Atrophy-induced changes in axonal cable properties (e.g., decreased unit area) and associated electrophysiological consequences, such as reduced conduction velocity (Sakaguchi *et al*., 1993; Yuan *et al*., 2009), could be responsible for the characteristic neurological deficits that accompany γ-diketone neuropathy; for example, gait abnormalities and hindlimb skeletal muscle weakness (Lehning *et al*., 2000). Based on the relative importance of NFs in determining axon caliber, we hypothesized that HD impaired NF maintenance (turnover) and thereby caused axon atrophy via the premature dissociation of these structures (LoPachin and DeCaprio, 2004, 2005). At the molecular level, HD is a relatively hard electrophile that forms 2,5-dimethylpyrrole adducts with nucleophilic ε-amine groups on lysine residues of various proteins (reviewed in LoPachin and DeCaprio, 2005). Accordingly, DeCaprio *et al*. (1997) showed that HD selectively formed pyrrole adducts with lysine residues located within KSP repeats on C-terminal (tail) regions of NFM and NFH subunit proteins. The KSP regions appear to mediate subunit insertion into the stationary polymer (Ackerley *et al*., 2003), and therefore, HD adduction of corresponding lysine residues could prevent the participation of affected subunits in cytoskeletal turnover.

Our hypothesis is based on evidence that lysine residues on NF proteins are the primary targets of HD. However, other cytoskeletal targets have been implicated by studies demonstrating the expression of HD neurotoxicity in animal species (crayfish) and transgenic mouse models that lack NFs (Sickles *et al*., 1994; Stone *et al*., 2001). Correspondingly, specific lysine residues on non-NF proteins have been shown to be critically involved in cytoskeletal structure and function. At physiological pH, the ε-amino group of lysine exists predominately in the protonated (+ 1; $pK_a = 10.5$) form. Consequently, this positively charged basic residue can mediate protein-protein associations through electrostatic interactions with negatively charged acidic amino acids (e.g., glutamate)

and/or phosphate moieties on binding domains of cognate proteins. For example, the processivity of the monomeric kinesin motor, KIF1A, is dependent upon the interactions of lysine-rich K-loops with glutamate residues on cognate binding domains of tubulin (Okada and Hirokawa, 2000). In addition, the primary amine side chains of lysine residues on certain cytoskeletal proteins are sites for posttranslational modifications such as acetylation or methylation, for example, Lys^{40} on α-tubulin (Iwabata *et al*., 2005). These modifications are enzyme mediated (e.g., lysine acetyltransferases) and appear to influence cytoskeletal stability and motor protein trafficking (Yang and Seto, 2008). Lysine residues also function as proton donors in the catalytic centers of many enzymes, for example, Lys^{609} of acetyl-CoA synthase (Yang and Gregoire, 2007). Clearly, lysine residues on both NF and non-NF proteins perform critical functions, and accordingly, the axonal cytoskeleton represents a target-rich environment for HD. Pyrrolylation of lysine residues result in the formation of hydrophobic moieties with consequential changes in protein solubility, electrostatic potential, and tertiary structure (reviewed in LoPachin and DeCaprio, 2004, 2005). These physiochemical alterations could render HD-modified proteins functionally impaired. Therefore, to identify potential non-NF targets in axon cytoskeleton, we characterized the effects of HD intoxication on protein-protein interactions in microtubule (Saxton, 1994; Vallee, 1982) and NF (Letterier *et al*., 1996) preparations.

MATERIALS AND METHODS

Reagents. HD (acetonylacetone, 97% pure), adenosine 5′-(β,γ-imido)triphosphate tetralithium salt, and general chemical supplies were purchased from Aldrich Chemical Company, Inc. (St Louis, MO). EDTA-free Protease Inhibitor Cocktail was purchased from Roche Applied Sciences (Indianapolis, IN). Antibodies (mAb) against cytoskeletal components, corresponding sources, and catalog numbers are listed in Table 1. Goat anti-mouse or anti-rabbit IgG conjugated to alkaline phosphatase and Western Blue (alkaline phosphatase substrate) were purchased from Promega Life Sciences (Madison, WI). Pre-made gels, NativeMark unstained protein standards, and HiMark prestained high–molecular weight (HMW) protein standards were purchased from Invitrogen Co. (Carlsbad, CA).

Treatment of animals and neurological testing. All aspects of this study involving intoxication of animals were in accordance with the *NIH Guide for Care and Use of Laboratory Animals* and were approved by the local animal care committee. Adult male Sprague-Dawley rats (250–275 g; Charles River Laboratories, Wilmington, MA) were housed individually in polycarbonate boxes, and drinking water and Purina Rodent Laboratory Chow (Purina Mills, Inc., St. Louis, MO) were available *ad libitum*. HD was administered by gavage to randomly assigned groups of rats ($n = 4$–6) according to one of two daily dose rates, 175 or 400 mg/kg/day. These dose rates were chosen based on extensive neurological, quantitative morphometric, and molecular studies of γ-diketone neuropathy; for example, see LoPachin *et al.* (2002), (2003), and (2004). HD was dissolved in 0.9% saline and was administered at 3 ml/kg/day. Age-matched control rats ($n = 4$–6) received an equivalent volume of saline by daily gavage. Rats were treated with HD until a moderate level of neurotoxicity was achieved: 175 mg/kg/day = 98 days and 400 mg/kg/day = 21 days.

For each HD dose rate, the onset and development of neurotoxicity were assessed by open field gait observations and by body weight changes determined twice per week (LoPachin *et al*., 2004). To evaluate gait and postural abnormalities, rats were placed in a clear Plexiglass box and were observed for 3 min. Following observation, a gait score was assigned from 1 to 4, where 1 = a normal, unaffected gait; 2 = a slightly abnormal gait (tip-toe walking, hindlimb adduction); 3 = moderately abnormal gait (obvious movement abnormalities characterized by dropped hocks and tail dragging); and 4 = severely abnormal gait (dragging hindlimbs and complete absence of rearing). Animals were then administered saline or HD by gavage. A trained observer who was not involved in animal care or gavage administration performed the neurological evaluations.

TABLE 1
List of Reagents and Sources

	Antigen	Clone	Company	Catalog number
Tubulin	α-Tubulin	DM1A	Sigma	T9026
	β-Tubulin	KMX-1	Millipore	MAB3408
Neurofilaments	NFH	3G3	Upstate	05-848
	NFM	3H11	Abcam	ab7256
	NFL	DA2	Abcam	Ab7255
Motor proteins	KIF1A	16/KIF1A	BD	612094
	KIF3A	—	Abcam	ab11259
	KIF5-HC	H2	Abcam	ab23664
	KIF5-LC	L2	Abcam	ab23586
	Dynein-HC	R-325	Santa Cruz	sc-9115
	Dynein-IC	70.1	Sigma	D5167
	Dynactin1	—	Novus	NBP1-0344
MAPs	MAP1A	HM-1	Millipore	MAB362
	MAP1B-HC	3G5	Abcam	ab3085
	MAP1B-LC	H-130	Santa Cruz	sc-25729
	MAP2	HM-2	Millipore	MAB364
	Tau (phos/non-phos)	Tau-5	Millipore	MAB361
Ubiquitin	Ubiquitin	—	Sigma	U5378

Taxol-stabilized microtubule motor protein preparation. To identify HD-induced changes in microtubule-cytoskeletal protein interactions, we used a taxol-stabilized microtubule motor protein assay (Saxton, 1994; Vallee, 1982) prepared from spinal cords of control or HD-intoxicated rats. The use of spinal cord preparations is based on quantitative morphometric and molecular evidence, suggesting that this CNS region is a neurotoxicologically relevant site of HD action; for example, see LoPachin *et al.* (2003), (2004), and (2005). Spinal cords (0.45 gm/rat) were rapidly excised and homogenized in 1.5 volumes of buffer (pH 7.4) containing (final concentrations) piperazine-N,N′-bis(2-ethanesulfonic acid) (PIPES) (100mM), $MgSO_4$ (1mM), ethylene glycol tetracetic acid (EGTA) (1mM), 2-mercaptoethanol (1mM), and protease inhibitor cocktail using a Potter-Elvehjem tissue grinder with a polytetrafluoroethylene (PTFE) pestle (5 strokes). The homogenate was centrifuged at 51,500 × g (Beckman JA-20.1 rotor) for 10 min to remove cellular debris. The pellet (P1) was discarded and the supernatant (S1) was centrifuged (51,500 × g) for an additional 2 h (4°C) to remove insoluble neurofilament polymer. The S2 supernatant was used for microtubule assembly by adding GTP (1mM), taxol (20μM), 2-mercaptoethanol (1mM), and PMSF (1mM). This solution was then incubated at 37°C for 20 min and either adenosine 5′-(β,γ-imido) triphosphate tetralithium salt (AMPPNP) (5mM) or ATP (2mM) was added, and the preparation was incubated for an additional 20 min (37°C). The microtubule assembly preparation was layered over a cushion buffer containing 10% sucrose, GTP (1mM), taxol (20μM), PIPES (100 mM), 2-mercaptoethanol (1mM), PMSF (1mM), and AMPPNP (5mM) or ATP (2mM) and then centrifuged at room temperature for 30 min at 21,000 × g (Micro21 rotor). The resulting gelatinous P3 pellet was dissolved in urea lysis (UL) buffer containing urea (7M), thiourea (2M), 3-(3-cholamidopropyl dimethylammonio)-1-propanesulfonic (4%), and dithiothreitol (10mM) by triturating through a 26-gauge needle. Both the pellet

(P3) and corresponding supernatant (S3) were stored (–80°C) for immunoblot analysis.

Neurofilament cosedimentation assay. To determine whether HD altered NF-cytoskeletal protein interactions, the NF cosedimentation assay of Letterier *et al.* (1996) was used. Spinal cords (0.45 gm/rat) were rapidly excised from control and HD-intoxicated rats (LoPachin *et al.*, 2004) and were homogenized in 1.0 volume of 2-(N-morpholino)ethanesulfonic acid (MES) buffer (pH 6.8) containing (final concentrations) MES (100mM), $MgSO_4$ (1mM), EGTA (1mM), AMPPNP (5mM) or ATP (2mM) and protease inhibitor cocktail using a Potter-Elvehjem tissue grinder with a PTFE pestle (6 strokes). The homogenate was centrifuged at 51,520 × g (Beckman JA-20.1 rotor) for 40 min, the supernatant (S1) was collected, and centrifuged (51,520 × g) for an additional 30 min. The S2 supernatant was mixed with glycerol (one-half supernatant volume) by trituration (20×) and then incubated for 3 h (4°C). Following incubation, the S2 fraction was centrifuged at 125,874 × g (Beckman TLA-45 rotor) for 1 h (4°C). The P3 pellet, which represented the aggregated neurofilament polymer, was collected and resuspended in 200 µl of UL buffer and was triturated through a 26-gauge needle (5×). The P3 pellet and corresponding S3 fractions were stored at −80°C.

Preparation of native protein complexes. Spinal cords (0.45 g/rat) from control and HD-treated rats were homogenized in 9 volumes of buffer (pH 6.8) containing (final concentrations) bis-tris (20mM), NaCl (20mM), digitonin (4.5mM), $MgCl_2$ (3mM), EDTA (0.5mM), EGTA (0.5mM), glycerol (10%), and protease inhibitor cocktail using a Potter-Elvehjem tissue grinder with a PTFE pestle (14 strokes). The homogenate was centrifuged at 20,000 × g (Beckman JA-20.1 rotor) for 30 min. The pellet was discarded and the supernatant was aliquoted and stored at −80°C.

Gel electrophoresis and semi-quantitative immunoblot analysis. To assess relative changes in the protein distribution of selected microtubule or NF cosedimentation fractions, protein samples from both control and experimental animals were separated on the same gel, 0.25–80 µg protein per lane. In general, tris-glycine continuous gradient gels (8–16%) were used to separate proteins. However, for separation of higher molecular weight complexes (> 100 kDa), tris-acetate gels (4–12%) were used. Protein contents were measured by the Bio-Rad protein assay. For high-resolution analysis of native protein complexes, the blue native PAGE technique was used. Supernatant (see above) was mixed with G-250 dye (5%) and was loaded onto NativePAGE Novex (3–12%) bis-tris gels. Following electrophoretic separation of native proteins or cosedimented fractions, proteins were transferred to polyvinylidene fluoride membranes overnight. After transfer, membranes were blocked with 5.0% dried milk in tris-buffered saline (TBS)/0.1% Tween 20 for 1 h and then rinsed. Membranes prepared from fractions were incubated for 1 h with a selected monoclonal antibody (Table 1) diluted in 5% dried milk/TBS. Following primary antibody incubation, membranes were washed in TBS and incubated (1 h) with AP-conjugated secondary antibody (goat anti-mouse or anti-rabbit IgG). Membranes were washed again and immunoreactive bands were visualized with alkaline phosphatase substrate (Western Blue). Immunoreactive cytoskeletal protein bands were scanned with a densitometer, digitized, and analyzed using the freehand selection tool of the NIH Imaging Program. Densitometric data were normalized to β-tubulin (which did not exhibit HD-induced changes) and are expressed as relative intensity (LoPachin *et al.*, 2004). To insure analysis within a linear range, initial studies established the proper electrophoresis protein loads, primary antibody dilutions, exposure duration, and band intensity levels for densitometric measurements (for details, see Chiu *et al.*, 2000).

Statistical methods. Experimental and control gait scores were compared using the Mann-Whitney *U*-test. *Post hoc* comparisons were performed using Dunnett test for comparison of each HD mean to its respective age-matched control mean (see Lehning *et al.* [2000] for methodological details). The respective relative band density data for individual cytoskeletal proteins in the HD exposure and age-matched controls group were compared using Duncan multiple range test ($p < 0.05$).

RESULTS

Neurological Status, Body Weight, and Cumulative HD Dose

Exposure to either HD dose rate (175 or 400 mg/kg/day) produced progressive gait abnormalities and a slowing of body weight gain (LoPachin *et al.*, 2002). Thus, by day 21 of the higher HD dose-rate regimen, mean (± SEM) gait score reached a moderate-to-severely affected level (3.3 ± 0.2). At this time point, rats intoxicated at the higher HD dose rate had gained 3% of their mean starting body weight (261 ± 7 g). In contrast, corresponding age-matched control rats had increased their mean (± SEM) starting body weight (269 ± 5 g) by 46%. A similar degree of neurotoxicity was induced by the lower daily dose rate, although the time to the neurological end point was relatively protracted; that is, moderate-to-severe neurological changes were achieved after 98 days of intoxication at 175 mg/kg/day (Table 2). At the completion of the lower dose-rate protocol (98 days), HD-intoxicated rats had gained 35% of their starting body weight (263 ± 4 g), whereas the age-matched control group increased their starting body weight (266 ± 5 g) by 107% (see LoPachin *et al.*, 2002, 2003, 2004). As reported previously (Lehning *et al.*, 1995, 2000), the cumulative dose of HD required to reach moderate-to-severe neurotoxicity was inversely related to the daily HD dose rate (Table 2).

Protein Distribution and ATP Release in Microtubule Motor Protein Preparations from Control Rat Spinal Cord

The taxol-stabilized microtubule polymer can be sedimented, and associated proteins were identified by immunoblot analysis. As expected, the tubulin proteins (e.g., β-tubulin) and KIF3 were highly enriched in control P3 fractions of microtubule motor protein preparations (Fig. 1). These proteins, however, were substantially less prevalent in the corresponding S3 supernatant. Instead, KIF1A (Fig. 1) and tau (data not shown) appeared to be relatively enriched in this fraction. Although the presence of NF subunits in the microtubule preparations (Fig. 1) could signify nonspecific contamination, it is more likely that they cosedimented with taxol-stabilized microtubules due to direct interactions with α,β-tubulin dimers (Bocquet *et al.*, 2009) and indirectly through their associations

TABLE 2
Neurological Status at End Point

Day	Gait score	Cumulative dose (g HD/kg)
98	3.5 ± 0.1*	17.2
21	3.3 ± 0.2*	8.4

Note. Data are expressed as mean ± SEM. 1 = Neurologically unaffected, 2 = slightly affected, 3 = moderately affected, and 4 = severely affected.
*Significantly different from respective control at $p < 0.05$.

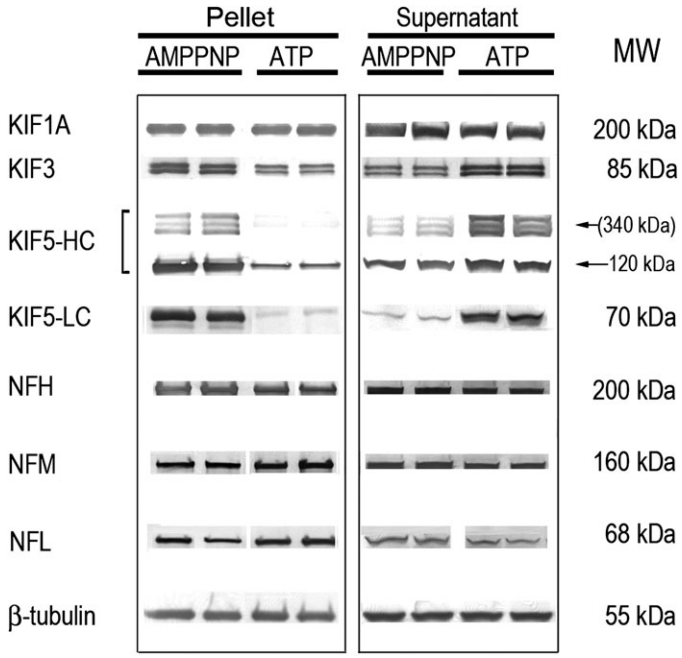

FIG. 1. Representative immunoblots are presented for kinesin motors and NF proteins in P3 pellets (left panel) and respective S3 supernatants (right panel) of control microtubule preparations. AMPPNP and ATP refer to the different protocols used for preparation of these fractions (see ''Materials and Methods'' section). Proteins were loaded on gels at 5–10 μg per lane. Respective MWs for individual proteins or peptides are presented to the right of the immunoblots. Relative to corresponding immunoblots from AMPPNP pellets, the reductions in KIF3 and KIF5 band densities in the ATP protocol indicate that these motor proteins were sensitive to ATP-induced release from microtubule binding. Upon release, the subsequently soluble KIF3 and KIF5 appear in the S3 supernatant, as evidenced by the corresponding increase in band densities, that is, compare ATP-derived data for pellet and supernatant. This study also demonstrates that the NF triplet proteins in the P3 pellet did not exhibit ATP sensitivity.

with motor proteins (kinesins, dynein) that provide bidirectional transportation along microtubule highways (Shah *et al.*, 2000; Wagner *et al.*, 2004).

The microtubule interactions of dimeric kinesin proteins are ATP dependent; for example, KIF3 can be released from microtubule binding in the presence of ATP (Gilbert *et al.*, 1995; Ikegami *et al.*, 2007). Correspondingly, AMPPNP, a nonhydrolyzable ATP analog, can be used to induce rigor binding of motors so that these proteins copurify with the microtubules (Scholey *et al.*, 1985). In our study, we determined the effects of ATP on protein distribution in spinal cord microtubule preparations from control and HD-intoxicated animals. Consistent with previous studies (e.g., see Ikegami *et al.*, 2007; Okada and Hirokawa, 2000), we found that the binding of the kinesins, KIF3 and KIF5, to microtubules in control preparations was significantly reduced in the presence of ATP. In contrast, the interactions of KIF1A (Fig. 1) and dynein (data not shown) were not sensitive (see Ikegami *et al.*, 2007). Thus, relative to the AMPPNP protocol, ATP reduced KIF3 microtubule binding by 45 ± 3% in the P3 pellet. The KIF5 heavy chain (HC)–immunopositive bands around 340 kDa and the corresponding native protein bands (120 kDa) were decreased by 90 ± 8% and 69 ± 5%, respectively (Fig. 1). The higher molecular weight variants (~340 kDa) recognized by the KIF HC antibody have been reported previously (e.g., Cuchillo-Ibanez *et al.*, 2008; Pfister *et al.*, 1989) and could represent cargo protein aggregates. The 70-kDa band detected by the KIF5 light chain (LC) antibody was reduced by 94 ± 7% in the ATP pellet fraction. As a result of ATP-induced protein detachment, corresponding increases of soluble KIF5 and KIF3 proteins were noted in the S3 supernatant (Fig. 1). Finally, our results demonstrate that the presence of NF subunits in the P3 fraction was insensitive to the ATP protocol (Fig. 1). This ATP-insensitive pool likely represents triplet proteins that bind directly to tubulin subunits (Bocquet *et al.*, 2009; Miyasaka *et al.*, 1993), as opposed to KIF5-bound NFs (Xia *et al.*, 2003).

Effects of HD Intoxication on Microtubule-Protein Interactions

HD intoxication was associated with changes in microtubule-protein interactions that were quantitatively similar in both the AMPPNP and ATP protocols. Therefore, Figure 2 presents data from the P3 pellet of the AMPPNP protocol only. Except where indicated, no significant HD-induced changes were noted in supernatant (S3) protein contents. Neither HD dose rate was associated with significant changes in the P3 tubulin (α,β) protein contents (Fig. 2). These data are consistent with previous studies (Chiu *et al.*, 2000; LoPachin *et al.*, 2004) and suggest that HD does not affect taxol-stabilized tubulin assembly. Although the anterograde kinesin motors, KIF1A and KIF3, were not affected, the 340-kDa band detected by the KIF5 HC antibody was selectively increased nearly 3-fold in both the supernatant (S3) and pellet (P3) from spinal cord of HD-intoxicated rats. This HC effect was ATP sensitive, which suggests that the increase was a compensatory rather than a toxic event, for example, involving protein cross-linking (see Discussion). Neither dynactin 1 nor dynein (HC or LC) were affected in HD samples (Fig. 2).

Regardless of the HD dose rate, the majority of microtubule-associated proteins (MAPs) tested exhibited substantial reductions in their respective P3 contents (Fig. 3). Thus, for example, in microtubule preparations from HD-intoxicated rats (400–175 mg/kg), the HC of MAP1B was reduced by 76 ± 10% to 63 ± 5%, respectively, when compared with control data, whereas the LC of MAP1B was not altered. No changes were noted in the respective supernatant (S3) fraction (data not shown). The NF native protein contents, that is, NFL, 68 kDa; NFM, 160 kDa, and NFH, 200 kDa, were not altered in the microtubule P3 fraction. However, consistent with previous findings in spinal cord preparations (LoPachin *et al.*, 2004), numerous HMW-immunoreactive NF species were prominent in the spinal cord pellet fraction from HD-treated rats (Fig. 4). These HMW species were less evident in control preparations (Fig. 4). Based on additional immunoblot analyses, the HMW

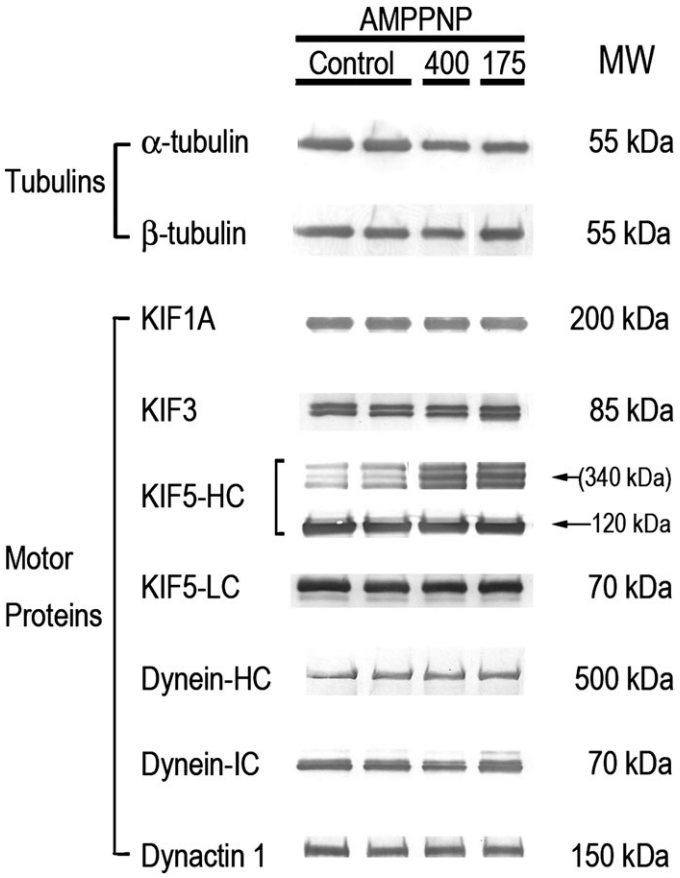

FIG. 2. Representative immunoblots are presented for tubulins and motor proteins in P3 pellets of control and HD (400 and 175 mg/kg/day dose rates) microtubule preparations. Proteins were loaded on gels at 0.25–10 μg per lane. The corresponding immunoblots from supernatant preparations did not reveal HD-induced changes in protein distribution (data not shown). AMPPNP refers to the protocol used for preparation of these fractions (see ''Materials and Methods'' section). Respective MWs for individual proteins or peptides are presented to the right of the immunoblots.

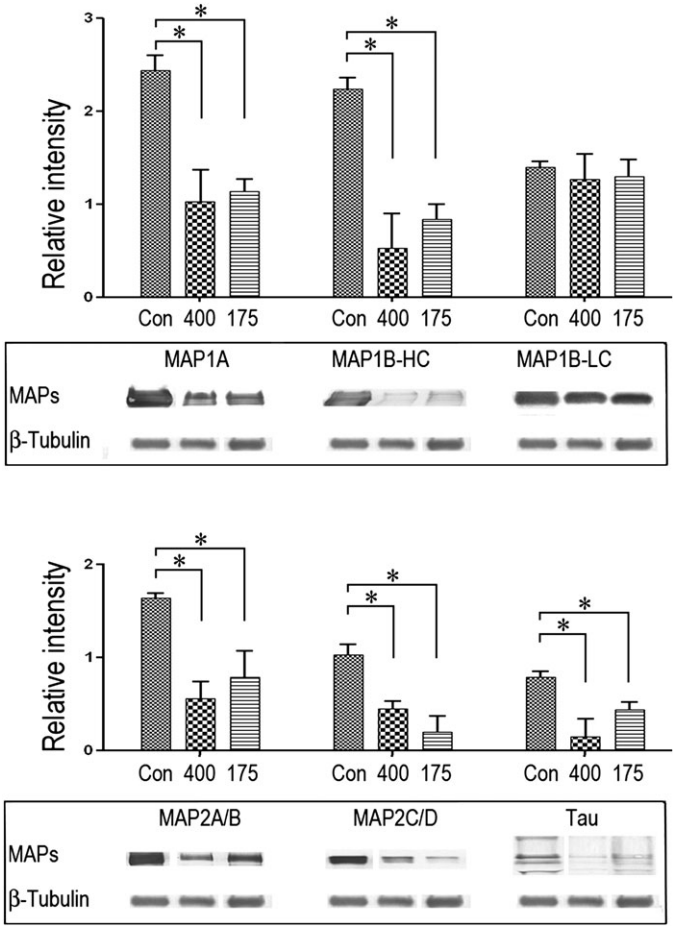

FIG. 3. Representative immunoblots are presented for MAPs in P3 pellets of AMPPNP microtubule preparations from control and HD (400 and 175 mg/kg/day)-intoxicated rats. Proteins were loaded onto gels at 0.25–20 μg per lane. Band intensities of the immunoblot data were quantified and normalized to ß-tubulin. Data are presented graphically as mean relative intensity (± SEM), and statistical differences between control and intoxicated group mean data are indicated by the connecting lines (*$p < 0.05$). The corresponding immunoblots from supernatant preparations did not reveal HD-induced changes in protein distribution (data not shown).

NF complexes did not appear to be consequences of ubiquitin binding (data not shown).

Effects of HD Intoxication on NF-Protein Interactions

NF proteins, like tubulin subunits, also interact extensively with other cytoskeletal proteins, for example, MAP2, KIF5A, dynein, and tubulin proteins (Bocquet *et al*., 2009; Wagner *et al*., 2004; Xia *et al*., 2003). Therefore, we used an NF-enriched cosedimentation assay to determine whether HD intoxication was associated with disrupted NF-protein interactions. Our results indicate that HD intoxication at either dose rate did not affect the distribution of tubulin, motor, or MAP proteins in the P3 or S3 fractions of the spinal cord NF preparations (data not shown). However, HMW NF species were abundant in the pellet, the molecular weight ranges of which were comparable to those observed in the microtubule preparations (see comparisons presented in Fig. 4). Figure 5 shows that these HMW NF complexes were normal components of the axon cytoskeleton. In nondenaturing conditions (native blue gels), varied HMW complexes are clearly evident in NF preparations (Fig. 5A). For each NF protein, the molecular weight distribution and corresponding densities of immunopositive bands were identical for both control and HD samples. In addition, several HMW NFL bands (e.g., 677 kDa, 636 kDa) of the native blue gels were common to NFH and NFM, suggesting that NFL can exist in hetero-oligomeric complexes with NFM or NFH. HMW species (up to 1211 kDa) were also identified for the HC of KIF5 (Fig. 5A). The corresponding immunopositive bands for this kinesin did not appear to correspond to any HMW NF band.

When proteins were separated in denaturing conditions (tris-acetate PAGE), detergent-insoluble HMW bands were detected for all NF proteins in both control and HD samples (Fig. 5B). These HMW species were present but not prevalent in control

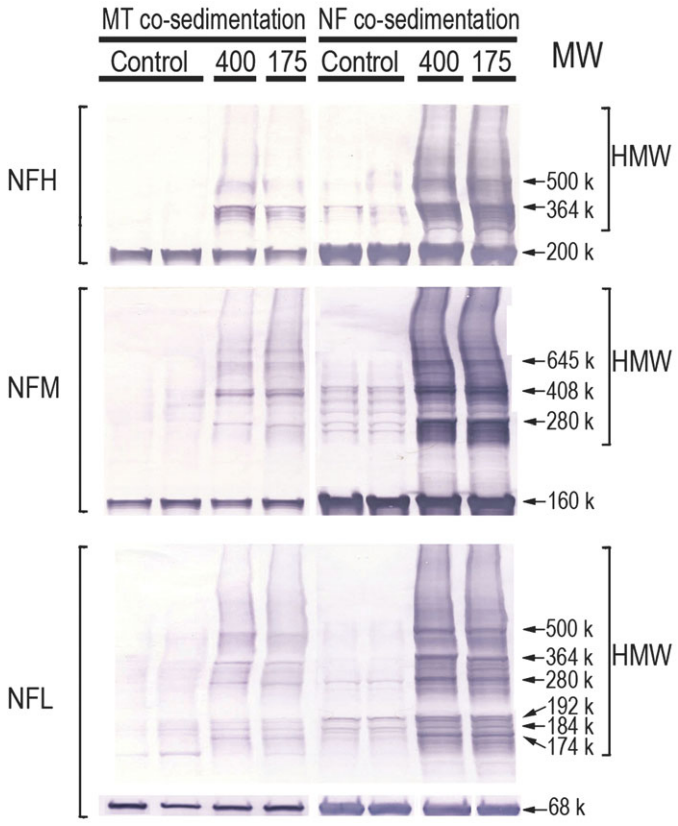

FIG. 4. Representative immunoblots are presented for NF proteins (NFH, NFM, and NFH) in the final pellet of microtubule or NF preparations from control and HD-intoxicated (400 and 175 mg/kg/day dose rates) rats. Proteins were loaded on gels at 15 μg per lane. Immunoblots from HD samples illustrate the HMW derivatives associated with each NF subunit. The HMW laddering pattern for each subunit was comparable regardless of preparation method (i.e., microtubule vs. NF). In addition, similar HMW bands are clearly evident in control samples from microtubule or NF preparations.

samples because they were detected only when corresponding protein concentrations were 5- to 10-fold higher than those used for HD samples. Similar to protein separation in nondenaturing conditions (Fig. 5A), cross-comparisons among NF proteins from control samples revealed several HMW NFL bands (e.g., 280 kDa, 364 kDa) that were common to both NFH and NFM. This suggests that NFL forms hetero-oligomeric complexes with NFM or NFH. The antibody for the KIF5 HC (Fig. 5B) detected several detergent-insoluble HMW bands. The KIF5 HC bands centered on 340 kDa corresponded to HMW NF bands. However, it is unlikely that this correspondence indicates an interaction (e.g., KIF5-NFL) because the HMW KIF5 bands were ATP sensitive and the comparable NF bands were not (see "Effects of HD Intoxication on Microtubule-Protein Interactions" section). When density scanning (NIH ImageJ) was used to compare the respective distributions of HMW NF-immunopositive bands from control and HD-intoxicated animals, substantial agreement was evident at the lower molecular weight ranges, for example, NFL $\leq$ 192 k and NFM $\leq$ 408 k (Fig. 6). However, at higher molecular weight ranges, control NF immunoblots exhibited less correspondence (fewer overlapping bands) to blots from HD-intoxicated rat, for example, NFL $\geq$ 192k and NFM $\geq$ 408 (Fig. 6).

DISCUSSION

Previous research has focused on NF subunit proteins as neurotoxicologically relevant sites of HD action (e.g., DeCaprio and Fowke, 1992; LoPachin *et al.*, 2004). However, in the present study, we used a cosedimentation approach to determine whether other components of the axon cytoskeleton might be involved. Results indicate that HD intoxication did not alter the presence of either α- or β-tubulin in high-speed pellet fractions of microtubule preparations. This suggests that HD does not affect taxol-stabilized tubulin assembly but does not exclude the possibility of altered tubulin polymerization in the absence of taxol (e.g., see Boekelheide, 1987). HD intoxication also was not associated with general changes in the pellet distribution of either anterograde (KIF1A, KIF3 or KIF5) or retrograde (dynein) molecular motors (Fig. 2). Nor was the cosedimentation of dynactin, a dynein-associated protein (Gill *et al.*, 1991), affected. The presence of tubulin and motor proteins was not changed in the corresponding high-speed supernatant (S3). Overall, these data indicate that HD did not alter the interactions of motor proteins with microtubules. Our studies do not address function directly. Nonetheless, the results suggest that HD did not affect the ATPase activity of KIF3 and KIF5, which should have caused rigor microtubule binding and the retention of these motors in the ATP protocol.

Immunoblot analyses of MAP proteins in microtubule preparations (P3) revealed substantial reductions (45–80%) in MAP1A, MAP 1B-HC, MAP2, and tau (Fig. 3) in spinal cord of HD-intoxicated rats. No changes in MAP protein content were evident in either the supernatant (S3) or the NF cosedimentation preparations. Although pair fed- and watered-control groups were not included in the present study, it is unlikely that the highly selective changes in MAP proteins represent nonspecific effects related to HD-imposed slowing of weight gain. It is also unlikely that these selective effects are due to taxol interference with MAP-microtubule interactions (Vallee, 1982) or reductions in gene expression. Our data, therefore, suggest that HD exposure specifically impaired MAP-microtubule binding, presumably through adduction of lysine residues that mediate such interactions. Although the toxicological consequences of this defect are unknown, decreased interfilament distances and loss of axon caliber are reasonable predictions. MAP proteins stabilize axonal/dendritic microtubules and regulate cytoskeletal interfilament distances (Chen *et al.*, 1992; Hirokawa, 1994). Consistent with defective MAP-based interfilament spacing, ultrastructural morphometric analyses of rubrospinal tract in HD-intoxicated rats demonstrated that loss of axon caliber was associated with increased

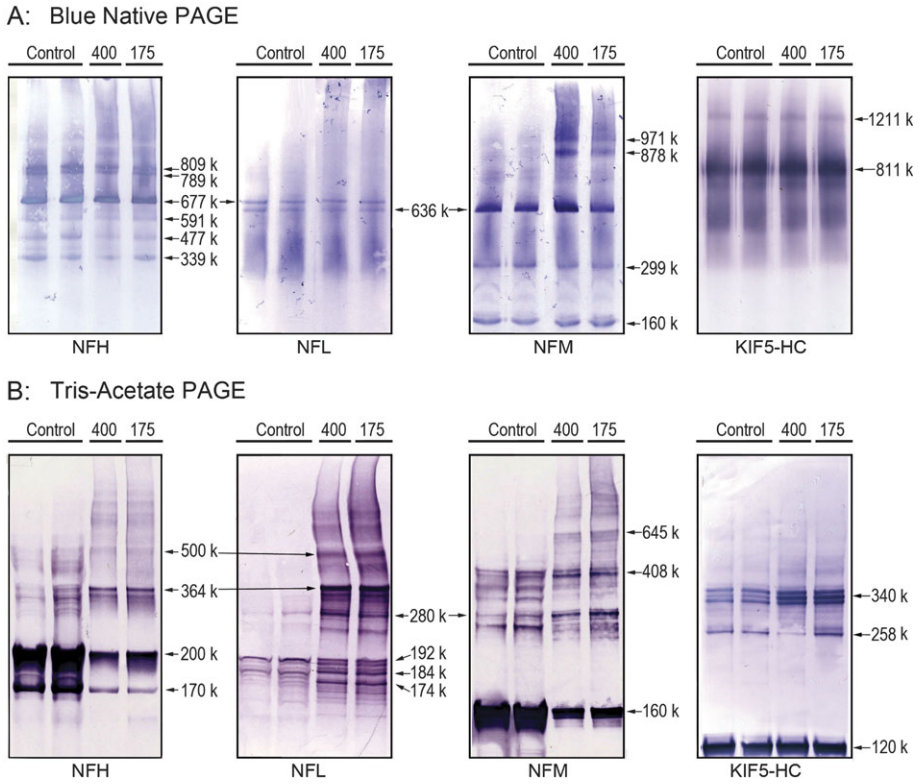

FIG. 5. Representative immunoblots are presented for NF proteins (NFH, NFM, and NFH) and KIF5-HC in NF preparations from control and HD-intoxicated (400 and 175 mg/kg/day dose rates) rats. (A) Immunoblots derived from proteins separated in nondenaturing gel conditions (Blue native PAGE). Proteins were loaded on gels at 50 μg per lane. (B) Immunoblots derived from proteins separated in denaturing gel conditions (tris-acetate/SDS-PAGE). Gels for NF immunoblots from HD samples were loaded at 2.5–5.0 μg protein per lane, whereas proteins from control samples were loaded at 25 μg per lane. Gels for kinesin immunoblots were loaded at 5 μg regardless of sample origin (control vs. HD).

microtubule density (LoPachin *et al*., 2005). Recent computer-based nearest neighbor analyses showed that mean (± SEM) microtubule-microtubule (MT-MT) distances were significantly decreased in rubrospinal axons, for example, control MT-MT distance = 13.15 ± 1.1 nm versus 9.80 ± 1.0 nm HD 400 mg/kg/day × 21 days (LoPachin, Zhang, and Gavin, unpublished data). Furthermore, as observed in HD neurotoxicity, *map2*$^{-/-}$ and *map1b*$^{-/-}$ knockout mouse models also exhibit axon atrophy, reduced nerve conduction velocity, microtubule condensation, and gait abnormalities (Edelmann *et al*., 1996; Teng *et al*., 2001). Microtubule perturbation due to decreased MAP interactions could lead to disrupted microtubule-based axonal transport. However, Teng *et al*. (2001) reported normal anterograde transport in *map2*$^{-/-}$ *map1b*$^{-/-}$ knockout mouse brain. Also seemingly inconsistent, HD intoxication was associated with selective acceleration of NF transport in CNS and PNS axons (reviewed in LoPachin and DeCaprio, 2004, 2005). Rather than being the result of a direct neurotoxic action, this effect is most likely secondary to the well-documented loss of stationary NFs (Monaco *et al*., 1989), which has been shown to accelerate the transport rate of NF proteins (Millecamps *et al*., 2007). Thus, reduced MAP-microtubule interactions could cause condensation of the axon cytoskeletal structure and lead to axon atrophy in HD-intoxicated animals.

Lysine-based electrostatic interactions govern the binding of many cytoskeletal proteins to the microtubule polymer, for example, kinesins, dyneins, and MAPs (Carter *et al*., 2008; Noble *et al*., 1989; Okada and Hirokawa, 2000). Therefore, in contrast to the observed selective effect on MAP distribution, a more generalized HD-induced disruption of microtubule-protein associations might be expected to accompany pyrrole-mediated lysine modifications. However, as quantum mechanical data presented in Table 3 indicate, HD is a relatively hard but weak electrophile that forms lysine adducts very slowly (see also DeCaprio *et al*., 1982). Consequently, the nucleophilicity of specific lysine residues will determine subsequent adduct formation (DeCaprio and Fowke, 1992). Thus, at physiological pH, the primary ε-amine group of lysine is protonated (+ 1) and, therefore, has very low nucleophilicity. In contrast, microenvironmental influences (e.g., vicinal acidic amino acids or phosphate moieties; Mukouyama *et al*., 2004) can lower the pK_a to the extent that a specific lysine exists in the more nucleophilic deprotonated state (0) at neutral pH. This state represents the preferential target at low *in vivo* HD concentrations. Whether the reduced MAP contents of our cosedimentation studies represent decreased microtubule binding due to pyrrole adduction of lysine residues will require on-going mass spectroscopic analyses. If adduct formation is involved, low pK_a

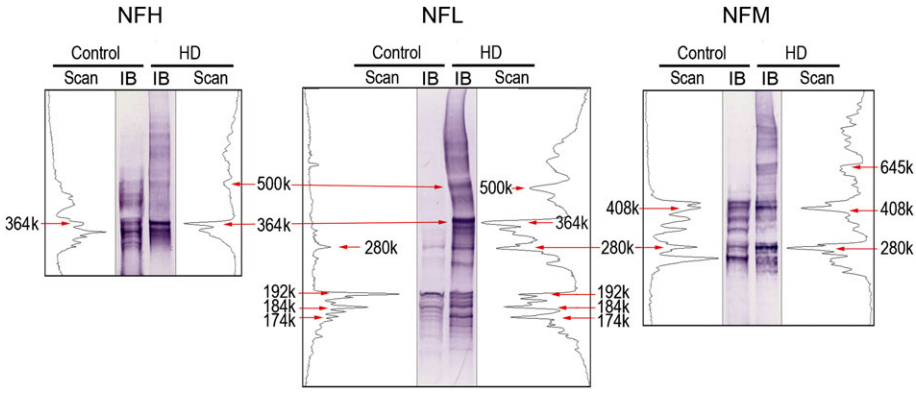

FIG. 6. For each NF subunit, representative lanes from Figure 5B are presented from a control and an HD immunoblot (IB). The respective density scans (NIH ImageJ) for the HMW NF-immunopositive bands are provided on either side of the corresponding immunoblot. The immunoblots were calibrated to the HiMark prestained HMW protein standards.

lysine residues on the MAPs or their cognate tubulin-binding domains will be the preferential targets. Conversely, our finding that HD intoxication does not alter the cytoskeletal interactions of motor proteins (Fig. 2) suggests that either lysine residues are not involved in these types of protein-protein associations or that the lysine ε-amine groups are in a low nucleophilic (+ 1) state that does not favor HD adduct formation.

Consistent with earlier studies (e.g., DeCaprio and O'Neill, 1985), HMW NF derivatives were identified in both the microtubule and NF co-sedimentation assays. These derivatives spanned a broad range of molecular weights (Fig. 4) and were more abundant in the pellet fraction than corresponding supernatant. HMW NF species in HD-intoxicated animals have been previously interpreted as cross-linked monomers: that is, pyrrole adduct formation at lysine residues is followed by oxidative reactions that yield pyrrole-pyrrole cross-linked proteins (reviewed in Graham *et al.*, 1991). However, this interpretation is based on *in vitro* chemical findings that have not been corroborated by proteomic evidence demonstrating the direct involvement of HD in the *in vivo* formation of HMW NF derivatives (reviewed in LoPachin and DeCaprio, 2005). Our results (Figs. 4 and 5), in conjunction with previous investigations (Gupta *et al.*, 2000; Karlsson *et al.*, 1991), indicate that HMW NF species are present in both control and HD preparations. The significant, although not complete, homology among respective HMW-immunopositive bands suggests that at least some of these complexes are normal cytoskeletal constituents that are elevated as a consequence of HD neurotoxicity. The exact protein composition of these detergent-insoluble NF complexes and their functional significance to axon physiology are both unknown. Nonetheless, our data (Figs. 5B and 6) suggest that certain HMW species (e.g., 500, 364, and 280 K) represent heterodimers and heterooligomers of NFL in combination with NFH or NFM subunits. It is therefore, possible that these NF complexes are transported units involved in maintenance of the stationary NF polymer (e.g., Millecamps *et al.*, 2007; Yuan *et al.*, 2003). However, the HMW NF complexes mediating cytoskeletal turnover are detergent soluble (Carden and Eagles, 1983; Cohlberg *et al.*, 1995), whereas the complexes identified in this and other studies are resistant to detergents (SDS), reducing agents (dithiothreitol), and proteolytic degradation (Heijink *et al.*, 2000). Alternatively, the formation of insoluble HMW NF complexes similar to those observed in the present study can be catalyzed by transglutaminase enzymes (Grierson *et al.*, 2001; Selkoe *et al.*, 1982). These are calcium-activated zymogens that form covalent ε-(γ-glutamyl)lysine bonds between proteins and thereby endow supramolecular structures, such as the cytoskeletal lattice, with extra rigidity and a resistance to proteolytic degradation (Lorand and Graham, 2003). Therefore, the low-level HMW NF derivatives observed in control spinal cord preparations might represent baseline levels of cytoskeletal proteins that have been cross-linked via the normal actions of axonal transglutaminases (e.g., TG2; Norlund *et al.*,

TABLE 3
Calculated Quantum Mechanical Parameters for Electrophiles

Electrophile	E_{LUMO} (eV)	E_{HOMO} (eV)	η	ω
n-Hexane	2.52	− 8.28	5.40	0.77
HD	− 0.44	− 6.70	3.13	2.04
Acrylamide	− 0.86	− 6.77	2.95	2.46
Acrolein	− 1.70	− 6.98	2.64	3.57

Note. LUMO, lowest unoccupied molecular orbital; HOMO, highest occupied molecular orbital. The LUMO energies (E_{LUMO}) and the HOMO energies (E_{HOMO}) were calculated using Spartan04 (version 1.0.3) software (Wavefunction, Inc., Irvine, CA). Global (whole molecule) hardness (η) was calculated as $\eta = (E_{LUMO} - E_{HOMO})/2$ and the electrophilicity index (ω) was calculated as $\omega = \mu^2/2\eta$, where μ is chemical potential of the electrophile and was calculated as $\mu = (E_{LUMO} + E_{HOMO})/2$ (for details, see LoPachin *et al.*, 2008). The ω parameter is a measure of the electrophilic reactivity of a given chemical. Data indicate that HD and parent hexacarbon are harder (higher η value) electrophiles than the α,β-unsaturated carbonyls, acrylamide, and acrolein. However, HD is a significantly weaker electrophile (lower ω value) than acrylamide or acrolein.

1999). Accordingly, the elevated presence of HMW NF complexes in HD samples might reflect excess fragmentation of the stationary cytoskeleton (Monaco *et al*., 1989). Alternatively, these HMW complexes could be a consequence of increased transglutaminase activity in response to homeostatic stimuli or an increased availability of substrate (i.e., lysine or glutamic acid residues) secondary to HD-induced changes in protein tertiary structure. Clearly, interpretation of the HMW NF species is complicated by our observation that at least some of these derivatives represent normal cytoskeletal constituents.

Our study, in conjunction with earlier research (LoPachin *et al*., 2004, 2005; Sickles *et al*., 1994; Stone *et al*., 2001; Tshala-Katumbay *et al*., 2009), suggests that axon atrophy involves HD targeting of multiple cytoskeletal proteins, for example, MAPs, NF triplet proteins, gelsolin, and α-internexin. However, acceptance of this developing axonopathic scenario requires additional research to identify relevant amino acid targets on cytoskeletal proteins and to conclusively define the structural and functional consequences of HD adduction. With respect to the HMW NF species, further research is needed to determine the mechanism of formation (e.g., HD cross-linked NF subunits, transglutaminated NF-protein complexes) and pathogenic significance (if any). Regardless, the multiplicity of molecular targets for HD is consistent with growing evidence that other electrophilic neurotoxicants (e.g., acrylamide, acrylonitrile) act by forming adducts with many critical proteins (e.g., N-ethylmaleimide-sensitive factor, SNAP-25). Distal axon regions are selectively vulnerable to electrophilic attack due to the uniquely slow turnover rate of corresponding targets and subsequent accumulation of adducted, dysfunctional proteins (reviewed in LoPachin *et al*., 2008).

FUNDING

National Institute of Environmental Health Sciences (RO1 ES07912-12 to R.M.L.).

REFERENCES

Ackerley, S., Thornhill, P., Grierson, A. J., Bronlees, J., Anerton, B. H., Leigh, P. N., Shaw, C. E., and Miller, C. C. J. (2003). Neurofilament heavy chain side arm phosphorylation regulates axonal transport of neurofilaments. *J. Cell Biol.* **161,** 489–495.

Bocquet, A., Berges, R., Frank, R., Robert, P., Peterson, A. C., and Eyer, J. (2009). Neurofilaments bind tubulin and modulate its polymerization. *J. Neurosci.* **29,** 11043–11054.

Boekelheide, K. (1987). 2,5-Hexanedione alters microtubule assembly. II. Enhanced polymerization of crosslinked tubulin. *Toxicol. Appl. Pharmacol.* **88,** 383–396.

Carden, M. J., and Eagles, P. A. M. (1983). Neurofilaments from ox spinal nerves. Isolation, disassembly, reassembly and cross-linking properties. *Biochem. J.* **215,** 227–237.

Carter, A. P., Garbarino, J. E., Wilson-Kubalek, E. M., Shipley, W. E., Cho, C., Milligan, R. A., Vale, R. D., and Gibbons, I. R. (2008). Structure and functional role of dynein's microtubule-binding domain. *Science* **322,** 1691–1695.

Chen, J., Kanai, Y., Cowan, N. J., and Hirokawa, N. (1992). Projection domains of MAP2 and tau determine spacings between microtubules in dendrites and axons. *Nature* **360,** 674–677.

Chiu, F. C., Opanashuk, L. A., He, D. K., Lehning, E. J., and LoPachin, R. M. (2000). γ-Diketone peripheral neuropathy. II. Neurofilament subunit content. *Toxicol. Appl. Pharmacol.* **165,** 141–147.

Cohlberg, J. A., Hajarian, H., Tran, T., Alipourjeddi, P., and Noveen, A. (1995). Neurofilament protein heterotetramers as assembly intermediates. *J. Biol. Chem.* **270,** 9334–9339.

Cuchillo-Ibanez, S. A., Byers, H. L., Leung, K., Ward, M. A., Anderton, B. H., and Hanger, D. P. (2008). Phosphorylation of tau regulates its axonal transport by controlling its binding to kinesin. *FASEB J.* **22,** 3186–3195.

DeCaprio, A. P., and Fowke, J. H. (1992). Limited and selective adduction of carboxyl-terminal lysines in the high molecular weight neurofilament proteins by 2,5-hexanedione in vitro. *Brain Res.* **586,** 219–228.

DeCaprio, A. P., Kinney, E. A., and Fowke, J. H. (1997). Regioselective binding of 2,5-hexanedione to high-molecular-weight rat neurofilament proteins in vitro. *Toxicol. Appl. Pharmacol.* **145,** 211–217.

DeCaprio, A. P., Olajos, E. J., and Weber, P. (1982). Covalent binding of a neurotoxic n-hexane metabolite: conversion of primary amines to substituted pyrrole adducts by 2,5-hexanedione. *Toxicol. Appl. Pharmacol.* **65,** 440–450.

DeCaprio, A. P., and O'Neill, E. A. (1985). Alterations in rat axonal cytoskeletal proteins induced by in vitro and in vivo 2,5-hexanedione exposure. *Toxicol. Appl. Pharmacol.* **78,** 235–247.

Edelmann, W., Zervas, M., Costello, P., Roback, L., Fischer, I., Hammarback, J. A., Cowan, N., Davies, P., Wainer, B., and Kucherlapati, R. (1996). Neuronal abnormalities in microtubule-associated protein 1B mutant mice. *Proc. Natl. Acad. Sci. U.S.A.* **93,** 1270–1275.

Gilbert, S. P., Webb, M. R., Brune, M., and Johnson, K. A. (1995). Pathway of processive ATP hydrolysis by kinesin. *Nature* **373,** 671–676.

Gill, S. R., Schroer, T. A., Szilak, I., Steuer, E. R., Sheetz, M. P., and Cleveland, D. W. (1991). Dynactin, a conserved, ubiquitously expressed component of an activator of vesicle motility mediated by cytoplasmic dynein. *J. Cell Biol.* **115,** 1639–1650.

Graham, D. G., Genter St. Clair, M. B., Amarnath, V., and Anthony, D. C. (1991). Molecular mechanisms of γ-diketone neuropathy. *Adv. Exp. Med. Biol.* **283,** 427–431.

Grierson, A. J., Johnson, G. V. W., and Miller, C. C. J. (2001). Three different human tau isoforms and rat neurofilament light, middle and heavy chain proteins are cellular substrates for transglutaminase. *Neurosci. Lett.* **298,** 9–12.

Gupta, R. P., Abdel-Rahman, A., Jensen, K. F., and Abou-Donia, M. B. (2000). Altered expression of neurofilament subunits in diisopropyl phosphorofluoridate-treated hen spinal cord and their presence in axonal aggregation. *Brain Res.* **878,** 32–47.

Heijink, E., Scholten, S. W., Bolhuis, P. A., and de Wolff, F. A. (2000). Effects of 2,5-hexanedione on calpain-mediated degradation of human neurofilaments in vitro. *Chem. Biol. Interact.* **129,** 231–247.

Hirokawa, N. (1994). Microtubule organization and dynamics dependent on microtubule-associated proteins. *Curr. Opin. Cell Biol.* **6,** 74–81.

Ikegami, K., Heier, R. L., Taruishi, M., Takagi, H., Mukai, M., Shimma, S., Taka, S., Hatanaka, K., Morone, N., Yao, I., *et al*. (2007). Loss of α-tubulin polyglutamylation in ROSA22 mice is associated with abnormal targeting of KIF1A and modulated synaptic function. *Proc. Natl. Acad. Sci. U.S.A.* **104,** 3213–3218.

Iwabata, J., Yoshida, M., and Komatsu, Y. (2005). Proteomic analysis of organ-specific post-translational lysine-acetylation and -methylation in mice by use of anti-acetyllysine and –methyllysine mouse monoclonal antibodies. *Proteomics* **5,** 4653–4664.

Karlsson, J.-E., Rosengren, L. E., and Haglid, K. G. (1991). Quantitative and qualitative alterations of neuronal and glial intermediate filaments in rat nervous system after exposure to 2,5-hexanedione. *J. Neurochem.* **57,** 1437–1444.

Lehning, E. J., Dyer, K. S., Jortner, B. S., and LoPachin, R. M. (1995). Axonal atrophy is a specific component of 2,5-hexanedione peripheral neuropathy. *Toxicol. Appl. Pharmacol.* **135,** 58–66.

Lehning, E. J., Jortner, B. S., Fox, J. H., Arezzo, J. C., Kitano, T., and LoPachin, R. M. (2000). γ-Diketone peripheral neuropathy. I. Quantitative morphometric analyses of axonal atrophy and swelling. *Toxicol. Appl. Pharmacol.* **165,** 127–140.

Letterier, J. F., Kas, J., Hartwig, J., Vegners, R., and Janmey, P. A. (1996). Mechanical effects of neurofilament cross-bridges. Modulation by phosphorylation, lipids, and interactions with F-actin. *J. Biol. Chem.* **271,** 15687–15694.

LoPachin, R. M., Barber, D. S., and Gavin, T. (2008). Molecular mechanisms of the conjugated α,β-unsaturated carbonyl derivatives: Relevance to neurotoxicity and neurodegenerative diseases. *Toxicol. Sci.* **104,** 235–249.

LoPachin, R. M., and DeCaprio, A. P. (2004). γ-Diketone central neuropathy: axon atrophy and the role of cytoskeletal protein adduction. *Toxicol. Appl. Pharmacol.* **199,** 20–34.

LoPachin, R. M., and DeCaprio, A. P. (2005). Protein adduct formation as a molecular mechanism in neurotoxicity. *Toxicol. Sci.* **86,** 214–225.

LoPachin, R. M., He, D., Reid, M. L., and Opanashuk, L. A. (2004). 2,5-Hexanedione-induced changes in the monomeric neurofilament protein content of rat spinal cord fractions. *Toxicol. Appl. Pharmacol.* **198,** 61–73.

LoPachin, R. M., Jortner, B. S., Reid, M. L., and Das, S. (2003). γ-Diketone central neuropathy: quantitative morphometric analysis of axons in rat spinal cord white matter regions and nerve roots. *Toxicol. Appl. Pharmacol.* **193,** 29–46.

LoPachin, R. M., Jortner, B. S., Reid, M. L., and Monir, A. (2005). γ-Diketone central neuropathy: quantitative analyses of cytoskeletal components in myelinated axons of the rat rubrospinal tract. *Neurotoxicology* **26,** 1021–1030.

LoPachin, R. M., and Lehning, E. J. (1997). The relevance of axonal swelling and atrophy to γ-diketone neurotoxicity. *Neurotoxicology* **18,** 7–22.

LoPachin, R. M., Lehning, E. J., Stack, E. C., Hussein, S. J., and Saubermann, A. J. (1994). 2,5-Hexanedione alters elemental composition and water content of rat peripheral nerve myelinated axons. *J. Neurochem.* **63,** 2266–2278.

LoPachin, R. M., Ross, J. F., Reid, M. L., Das, S., Mansukhani, S., and Lehning, E. J. (2002). Neurological evaluation of toxic axonopathies in rats: acrylamide and 2,5-hexanedione. *Neurotoxicology* **23,** 95–110.

Lorand, L., and Graham, R. M. (2003). Transglutaminases: crosslinking enzymes with pleiotropic functions. *Nat. Rev. Mol. Cell Biol.* **4,** 140–156.

Millecamps, S., Gowing, G., Corti, O., Mallet, J., and Julien, J. P. (2007). Conditional NF-L transgene expression in mice for in vivo analysis of turnover and transport rate of neurofilaments. *J. Neurosci.* **27,** 4947–4956.

Miyasaka, H., Okabe, S., Ishiguro, K., Uchida, T., and Hirokawa, N. (1993). Interaction of the tail domain of high molecular weight subunits of neurofilaments with the COOH-terminal region of tubulin and its regulation by τ protein kinase II. *J. Biol. Chem.* **268,** 22695–22702.

Monaco, S., Autilio-Gambetti, L., Lasek, R. J., Katz, M. J., and Gambetti, P. (1989). Experimental increase of neurofilament transport rate: decreases in neurofilament number and in axon diameter. *J. Neuropathol. Exp. Neurol.* **48,** 23–32.

Mukouyama, S. B., Oguchi, M., Kodera, Y., Maeda, T., and Suzuki, H. (2004). Low pKa lysine residues at the active site of sarcosine oxidase from *Corynebacterium* sp. U-96. *Biochem. Biophys. Commun.* **320,** 846–851.

Noble, M., Lewis, S. A., and Cowan, N. J. (1989). The microtubule binding domain of microtubule-associated protein MAP1B contains a repeated sequence motif unrelated to that of MAP2 and tau. *J. Cell Biol.* **109,** 3367–3376.

Norlund, M. A., Lee, J. M., Zainelli, G. M., and Muma, N. A. (1999). Elevated transglutaminase-induced bonds in PHF tau in Alzheimer's disease. *Brain Res.* **851,** 154–163.

Okada, Y., and Hirokawa, N. (2000). Mechanism of the single-headed processivity: diffusional anchoring between the K-loop of kinesin and the C terminus of tubulin. *Proc. Natl. Acad. Sci. U.S.A.* **97,** 640–645.

Pfister, K. K., Wagner, M. C., Stenoien, D. L., Brady, S. T., and Bloom, G. S. (1989). Monoclonal antibodies to kinesin heavy and light chains stain vesicle-like structures, but not microtubules, in cultured cells. *J. Cell Biol.* **108,** 1453–1463.

Sakaguchi, T., Okada, M., Kitamura, T., and Kawasaki, K. (1993). Reduced diameter and conduction velocity of myelinated fibers in the sciatic nerve of a neurofilament-deficient mutant quail. *Neurosci. Lett.* **153,** 65–68.

Saxton, W. M. (1994). Isolation and analysis of microtubule motor proteins. *Methods Cell Biol.* **44,** 279–288.

Scholey, J. M., Porter, M. E., Grissom, P. M., and McIntosh, J. R. (1985). Identification of kinesin in sea urchin eggs, and evidence for its localization in the mitotic spindle. *Nature* **318,** 483–486.

Selkoe, D. J., Abaham, C., and Ihara, Y. (1982). Brain transglutaminase: in vitro crosslinking of human neurofilament proteins into insoluble polymers. *Proc. Natl. Acad. Sci. U.S.A.* **79,** 6070–6074.

Shah, J. V., Flanagan, L. A., Janmey, P. A., and Leterrier, J.-F. (2000). Bidirectional translocation of neurofilaments along microtubules mediated in part by dynein/dynactin. *Mol. Biol. Cell* **11,** 3495–3508.

Sickles, D. W., Pearson, J. K., Beall, A., and Testino, A. (1994). Toxic axonal degeneration occurs independent of neurofilament accumulation. *J. Neurosci. Res.* **39,** 347–354.

Stone, J. D., Peterson, A. P., Eyer, J., Oblak, T. G., and Sickles, D. W. (2001). Neurofilaments are nonessential to the pathogenesis of toxicant-induced axonal degeneration. *J. Neurosci.* **21,** 2278–2287.

Teng, J., Takei, Y., Harad, A., Nakata, T., Chen, J., and Hirokawa, N. (2001). Synergistic effects of MAP2 and MAP1B knockout in neuronal migration, dendritic outgrowth, and microtubule organization. *J. Cell Biol.* **155,** 65–76.

Tshala-Katumbay, D., Monterroso, V., Kayton, R., Lasarev, M., Sabri, M., and Spencer, P. (2009). Probing mechanisms of axonopathy. Part II: protein targets of 2,5-hexanedione, the neurotoxic metabolite of the aliphatic solvent n-hexane. *Toxicol. Sci.* **107,** 482–489.

Vallee, R. B. (1982). A taxol-dependent procedure for the isolation of microtubules and microtubule-associated proteins (MAPs). *J. Cell Biol.* **92,** 435–442.

Wagner, O. I., Ascano, J., Tokito, M., Leterrier, J.-F., Janmey, P. A., and Holzbaur, E. L. F. (2004). The interaction of neurofilaments with the microtubule motor cytoplasmic dynein. *Mol. Biol. Cell* **15,** 5092–5100.

Xia, C.-H., Roberts, E. A., Her, L.-S., Liu, X., Williams, D. S., Cleveland, D. W., and Goldstein, L. S. B. (2003). Abnormal neurofilament transport caused by targeted disruption of neuronal kinesin heavy chain KIF5A. *J. Cell Biol.* **161,** 55–66.

Yang, X.-J., and Gregoire, S. (2007). Metabolism, cytoskeleton and cellular signaling in the grip of protein N^{ε}-and O-aceltylation. *EMBO Rep.* **8,** 556–562.

Yang, X.-J., and Seto, E. (2008). Lysine acetylation: Codified crosstalk with other posttranslational modifications. *Cell* **31,** 449–461.

Yuan, A., Rao, M. V., Kumar, A., Julien, J.-P., and Nixon, R. A. (2003). Neurofilament transport in vivo minimally requires hetero-oligomer formation. *J. Neurosci.* **23,** 9452–9458.

Yuan, A., Rao, M. V., Sasaki, T., Rao, M. V., Kumar, A., Kanumuri, V., Dunlop, D. S., Liem, R. K. H., and Nixon, R. A. (2009). Neurofilaments form a highly stable stationary cytoskeleton after researching a critical level in axons. *J. Neurosci.* **29,** 11316–11329.